Physically-Based Modeling of Hand-Assembled Wire Bundles for Accurate EMC Prediction

Xiaokang Liu, Flavia Grassi, *Senior Member, IEEE,* Giordano Spadacini, *Senior Member, IEEE,* and Sergio A. Pignari, *Fellow, IEEE.*

***Abstract*—In this paper, a new modeling approach to generate wire bundles with geometry accurately mimicking the random displacements of the wires in real, hand-assembled bundles is proposed. To this end, the wire trajectories are modeled by three-dimensional curves that retain continuity of the wire path and its first derivative, allow enforcing random fluctuations of wire position in the bundle cross-section and controlling bundle density. An iterative algorithm involving both local and global perturbation of initially-generated trajectories is used to prevent wire overlapping. As a whole, the proposed modeling approach is able to reproduce (through the use of a limited number of parameters) the main physical properties of real hand-assembled wire bundles. In order to get either deterministic or statistical estimates of the EMC performance, the obtained bundle geometry can be easily imported into 3D electromagnetic solvers or modeled as a Multiconductor Transmission Line (MTL) by approximating the nonuniform wire paths as a sequence of uniform cascaded sections. Application examples aimed at the prediction of crosstalk and field-to-wire coupling are used to prove the importance of accurate modeling of the bundle geometry and proper digitization of the bundle along its length for prediction at high frequencies of the electromagnetic noise induced in the terminal units.**

***Index Terms*—Crosstalk, Field-to-Wire Coupling, Non-Uniform Transmission Lines, Random Wire Bundles.**

I. Introduction

RANDOMLY bundling wires and/or twisted-wire pairs in tightly-packed harnesses is a common practice in many industrial sectors, such as automotive and aerospace [1], [2]. From the Electromagnetic Compatibility (EMC) viewpoint, modeling these structures is challenging since the inherently-random geometry of such hand-made wiring structures quite often reflects into a large sensitivity of the noise induced (by crosstalk or field-to-wire coupling) at the entry points of the units connected to the harness ends.

Over the last decades, several contributions [1]–[8] have been proposed, aimed at providing effective representation of the bundle geometry, while retaining its inherently random nature. The *Random Midpoint Displacement* (RMD) algorithm [3], [4] was among the first attempts to describe randomness of the wire trajectories. This method foresees to subdivide the bundle into n uniform cascaded segments, and to represent wire positions by means of fractal curves. Wire continuity within the bundle is controlled through the fractal dimension and the total number of segments. However, the wires generated by this approach may exhibit discontinuities between adjacent segments, due to the use of an anti-overlapping algorithm acting locally. To reduce wire discontinuity along the bundle length and speed-up the computation of per-unit-length parameters, the *Random Displacement Spline Interpolation* (RDSI) algorithm was proposed, in [5]. This method involves cubic-spline interpolation across adjacent bundle segments and subsequent re-mapping of actual wire positions into pre-defined reference cross-sections to prevent wire overlapping along the bundle axis. This approach provides a better representation of the wire paths, but the transitions between adjacent segments still involve discontinuities as large as the wire diameter. Use of a unique (reference) cross-section for the bundle was adopted also in more recent works in combination with different algorithms to manage wire interchanges, [1], [2], [6]–[8]. Among these, the solution proposed in [1], [2] resorts to graph theory and to the concept of cycle to generate a data-base of all the possible wire interchanges, assuring minimum-distance wire movements across adjacent segments. However, in spite of undoubted advantages especially in the computation of the p.u.l. parameter matrices, the assumption of a constant cross-section leads to wire trajectories exhibiting discontinuities that cannot be reduced to less than one wire diameter. In the standing wave region, such discontinuities affecting the bundle geometry may result in fictitious signal reflections, giving rise to spurious resonances in the frequency response of the voltages and currents across the ports of the terminal units.

To overcome these limitations, a novel modeling approach is proposed in this paper, foreseeing representation of the wire trajectories in terms of analytical expressions, which guarantee smoothness of the wire paths and control of bundle density, avoiding wire overlapping at the same time. To assure compactness and incorporate bundle randomness, a suitable sub-set of the possible cycles introduced in [1] is used for the generation of possible wire interchanges. Wire continuity is assured by the use of cubic Hermite interpolating polynomials, which offer the advantage to avoid unphysical oscillations between sample points (this is not possible if spline interpolation is adopted). In the practically-relevant case of tight wire bundles, occurrence of wire overlapping is prevented by an *ad hoc* algorithm, which foresees first to project the wire trajectories onto a suitable set of basis functions, and then to iteratively perturb them yet retaining bundle compactness and wire continuity. As proven by the application examples, the generated bundle geometries can be successfully used to

X. Liu, F. Grassi, G. Spadacini, and S. A. Pignari are with the Department of Electronics, Information and Bioengineering, Politecnico di Milano, 20133 Milan, Italy, e-mail: xiaokang.liu@polimi.it; flavia.grassi@polimi.it; giordano.spadacini@polimi.it; sergio.pignari@polimi.it

predict EMC performance of hand-assembled bundles either in combination with 3D full-wave numerical solvers or with multi-conductor transmission line (MTL) models, approximating the overall bundle as the cascade of uniform sections. This latter approach will be hereinafter referred to as *Uniform Cascaded Sections* (UCS) method, [9]–[11]. Crosstalk and field-to-wire coupling predictions are illustrated with the intent to show the need for physically-based modeling of the bundle geometry and adequate digitization of the wire paths, as far as accurate EMC prediction in a wide frequency range is the target.

The manuscript is organized as follows. In Sec. II, physical constraints to assure smoothness and compactness of the generated wire harness as well as to avoid wire overlapping are introduced. The main features of the algorithms proposed for bundle generation are presented in Sec. III, and their application in the perspective of statistical estimation of EMC performance is discussed. In Sec. IV and Sec. V, the generated bundle geometry is used in combination with full-wave and MTL-based simulation for accurate prediction of crosstalk and field-to-wire coupling, respectively. Conclusions are eventually drawn in Sec. VI.

II. Physical Constraints

With reference to Fig. 1, the position of wire i, $i = 1,\ldots,N$, inside a bundle composed of N wires can be described by the trajectory of its center through a 3-dimensional curve $f_i(x_i, y_i, z), i = 1,\ldots,N, z \in [0,\ell]$, where z denotes the bundle longitudinal axis (common to all wires, and laying at constant height $x = h$ above a metallic ground plane), and (x_i, y_i) are the wire coordinates in the transverse (x, y) plane.

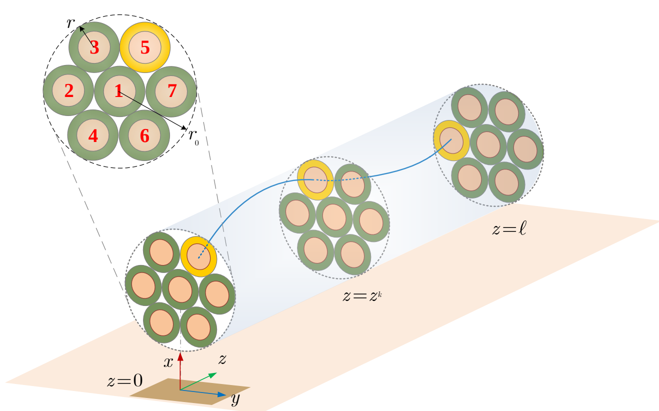

Fig. 1. Schematic representation of a random wire bundle. The blue curve is the spatial trajectory of a wire, whereas z denotes the longitudinal axis

At a given longitudinal coordinate z, $z \in [0,\ell]$, the pairwise distance between the centers of wire i and j $(i,j = 1,\ldots,N; i < j)$ is denoted by

$$d_{ij}(z) = \sqrt{[x_i(z) - x_j(z)]^2 + [y_i(z) - y_j(z)]^2} \quad (1)$$

According to the common practice, all wires in the bundle are assumed to have the same external radius $r_i = r$, $i = 1,\ldots,N$. Hence, the *non-overlapping constraint* for all wires inside the bundle writes

$$2r \leq d_{ij}(z), \; i,j = 1,\ldots,N; i < j \quad (2)$$

Such a constraint shall be satisfied for any longitudinal coordinate $z \in [0,\ell]$.

To retain wire smoothness, a *continuity constraint* of wire trajectories is introduced, by enforcing wire projections in the (z,x) and (y,z) planes, $x_i(z)$ and $y_i(z), i = 1,\ldots,N, z \in [0,\ell]$, to be continuous with respect to z. In mathematical terms, this condition requires that for any $z_0 \in (0,\ell)$, wire coordinates $x_i(z)$ and $y_i(z)$ satisfy

$$\begin{aligned} \lim_{z\to z_0^+} x_i(z) &= \lim_{z\to z_0^-} x_i(z) = x_i(z_0) \\ \lim_{z\to z_0^+} y_i(z) &= \lim_{z\to z_0^-} y_i(z) = y_i(z_0) \end{aligned} \quad (3)$$

Wires compactness along the bundle can be rendered by relying on the fact that the overall bundle cross-section exhibits pseudo-circular shape, especially when lacing cords are used to assure bundle compactness. Hence, a circular contour (centered at height $x = h$) is hereinafter introduced, hosting all the N wires in the bundle at each cross section along its length. By denoting with r_0 the maximum radius of such a circular contour, the *compactness constraint* writes

$$\sqrt{[x_i(z) - h]^2 + y_i^2(z)} + r \leq r_0 \quad (4)$$

By virtue of the modeling approach described above, generation of a bundle geometry mimicking the main physical features of real hand-assembled harness reduces to the search for a set of projection functions $x_i(z)$ and $y_i(z)$ simultaneously satisfying the *non-overlapping* (2), *continuity* (3) and *compactness* (4) constraints. Once these functions are found, the bundle geometry is fully determined, and the cross section at any position along the bundle can be extracted from the analytical expression of the wire paths.

III. Generation of the Bundle Geometry

In this section, two algorithms for the generation of the bundle geometry are presented, which incorporate the mathematical constraints introduced in Sec. II. The first algorithm does not avoid wire overlapping along the bundle length. Hence, it can be used for the generation of loose bundles only (specific conditions in terms of minimum wire-to-wire distance will be given in the following). The second algorithm overcomes such a limitation by embedding a suitable anti-overlapping scheme. Hence, it allows generation of tight bundle geometries without any restrictions on the minimum wire-to-wire distance. In both algorithms, wire positioning in every cross-section is optimized by resorting to packing problem theory [12], so to assure bundle compactness (i.e., a circular contour, see Sec. II, with minimum radius).

A. Algorithm for Loose Bundles of Wires

The first algorithm is based on piece-wise polynomial interpolation among random cross-sections assigned at n reference positions z_n along the bundle length (see Fig. 1). Namely, the trajectory of the $i-th$ wire is described by the x and y coordinates with expression:

$$x_i(z) = \begin{cases} x_{i0}(z) & z \in [z_0, z_1] \\ x_{i1}(z) & z \in [z_1, z_2] \\ \vdots & \\ x_{i(n-1)}(z) & z \in [z_{n-1}, z_n] \end{cases} \tag{5}$$

where $x_{ik}\,(k = 1, \dots, n-1)$ are polynomial functions, and $z_0, z_1, \dots, z_n$ denote the reference cross-section positions along the longitudinal $z-$axis. Similar expressions, here omitted for brevity, hold for the y coordinate. To evaluate the piece-wise functions, spline interpolation is a solution commonly adopted, [13], due to easy implementation and low-order (cubic) expressions. However, in this work use of piecewise cubic Hermite interpolating polynomials [14] is preferred, since this allows eliminating unphysical oscillations between sample points possibly introduced by spline interpolation (see Fig. 2 for an explicative example).

The proposed algorithm for the generation of the bundle geometry encompasses the following three steps.

1) *Generation of the reference cross-sections*. Given the number of wires within the bundle, wire positioning is optimized by the packing problem theory [12], and a circular contour with minimum radius is evaluated. A suitable number of subsections in which the bundle can be subdivided is (averagely) estimated based on inspection of the actual bundle realization. Without loss of generality, in the following examples, bundle sections with equal length are assumed, even if the proposed algorithm is general and can also manage bundles with sections of different length. Then, all possible cross-sections are generated by resorting to Graph Theory and the concept of cycle, so to assure minimum-distance movement of wires between adjacent cross-sections [1]. Once the complete set of cycles is evaluated (the number of possible cycles is reported in the second column of Tab. I), the cycles involving wire interchange between adjacent cross-sections are excluded, since in real hand-assembled bundles half-twist rotation between adjacent sections looks unphysical. Hence, the actual number of possible cycles shrinks, as shown in the third column of Tab.I.

2) *Interpolation between reference cross-sections*. Once a set of reference cross-sections is selected at random, the piece-wise interpolation algorithm is applied to the x- and y-coordinates of each wire in the bundle. This yields piece-wise polynomial functions with variable z, describing the trajectories of the N wires in the bundle. These positions are different from those initially set in the reference cross-sections, in contrast to [1] where merely fixed positions are available for each wire.

3) *Inspection of the generated bundle*. The obtained piece-wise polynomial curves are eventually inspected to check if the *non-overlapping* constraint is satisfied over the path of each wire. The *continuity* and *compactness* constraints do not require any a posteriori verification, since they are automatically satisfied by the algorithm.

TABLE I
TOTAL NUMBER OF POSSIBLE CYCLES

# wires	# cycles (all)	# cycles (no wire-interchanges)
2	2	1
3	6	3
4	14	7
5	31	13
6	64	21
7	212	63
8	456	121
9	893	201
10	1,769	347
11	3,448	587
12	6,933	997
13	12,363	1,561
14	45,567	5,027
15	152,075	15,417
16	502,499	46,729
17	1,661,436	141,631
18	5,439,076	429,339
19	16,043,600	1,215,717

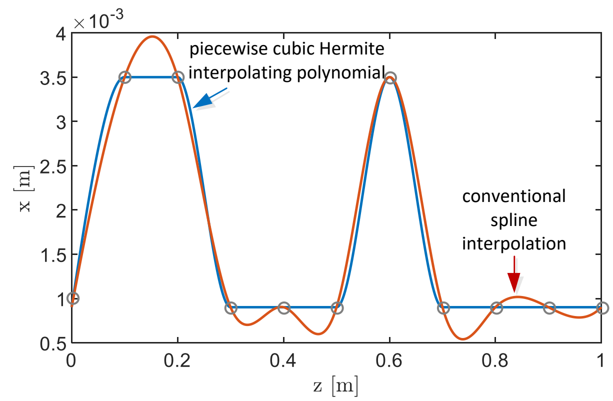

Fig. 2. Oscillations between sample points introduced by traditional spline interpolation w.r.t. the proposed piecewise cubic Hermite polynomials interpolation. For clarity, only the x coordinate of a wire path is plotted versus z. The sample points (circles) are separated by 10 cm, the bundle length is 1 m.

Since the proposed algorithm is not able to inherently prevent wire overlapping, the set of generated wire paths can be accepted as is only on condition that wire separation is sufficiently large. To investigate the possible occurrence of wire overlapping as a function of the minimum wire separation s (i.e., separation $s = \min(d_{ij})$ between wires), a large number $(10,000)$ of bundle samples with different s/r ratio were randomly generated and inspected. The survey led to estimate $s/r = 6$ as the threshold value above which wire overlapping does not occur (see Fig. 3). Hence, the inspection step (step 3 in the above described algorithm) can be omitted for $s/r > 6$. Conversely, for s/r approximately smaller than 4.5, the proposed procedure for bundle generation fails, since a very high probability of wire overlapping was observed. The enhanced algorithm proposed in the next paragraph overcomes such a limitation, and enables bundle generation of even very tight random bundles yet avoiding wire overlapping.

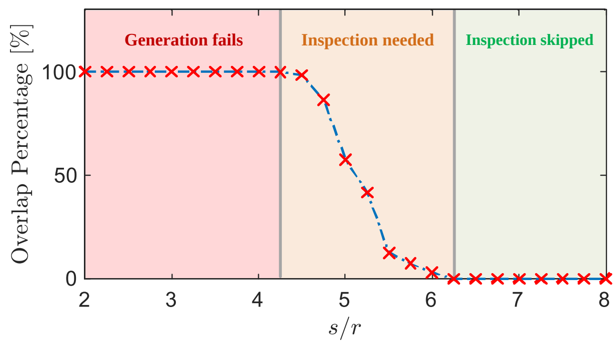

Fig. 3. Wire overlapping occurrence percentage versus s/r ratio for a 1 m-long bundle with $N = 7$ conductors and 10 sub-sections of longitudinal length $L_s = 10$ cm.

B. Algorithm for Tight Bundles of Wires

Generation of (more realistic) tight bundle geometries involves circle packing and optimal spatial search problems. To the best of the Authors' knowledge, no efficient algorithms are currently available in the technical literature for this bundle category.

The method here proposed is based on the idea to convert wire trajectories into coefficient matrices. Accordingly, the x- and y-trajectories of the $i-th$ wire can be expressed in terms of higher order polynomial functions (or, as an alternative, of Fourier series coefficients) with respect to the longitudinal coordinate z. In compact form, they write:

$$x_i = \mathbf{C}_i^{(x)} \mathbf{b}_i^{(x)}(z)\,; \;\; y_i = \mathbf{C}_i^{(y)} \mathbf{b}_i^{(y)}(z) \tag{6}$$

where $\mathbf{C}_i^{(x,y)}$ denote the matrix entries of the $i-th$ wire, and $\mathbf{b}_i^{(x,y)}(z)$ are the corresponding basis functions.

In order to obtain a valid set of coefficients in (6) with a predefined polynomial function vector, the proposed algorithm generates an initial guess for the bundle trajectories starting from the reference cross-sections introduced in Sec. III.A (see the first step of the previously-described procedure). The preliminary basis functions (e.g., $\mathbf{b}_i^{(x,y)} = \left[1, z, z^2, \ldots, z^M\right]^t$) are determined by numerical computational methods, so to assure wire smoothness. Within this initial step, possible wire overlapping is temporarily neglected. Afterwards, these initial trajectories are locally and iteratively perturbed, by enforcing the twofold constraint of minimum wire movement and non-overlapping, and by accordingly adjusting the coefficient matrices $\mathbf{C}_i^{(x,y)}$ for each wire i. Once all the conductors have been perturbed, a final check ensures that the bundle is properly fitted into polynomial functions. The above procedure is iterated until the obtained polynomial representation satisfactory retains all the physical constraints in Sec. II.

Two examples of wire bundles generated via the proposed algorithm are shown in Fig. 4. Both bundles are composed of $N = 19$ conductors, and are sub-divided into 4 sections. The loose bundle in Fig. 4(a) is characterized by wire separation $s = 6r$, and was generated by the algorithm in Sec. III.A. The tight bundle in Fig. 4(b) is characterized by wire separation $s = 2.5r$, and was generated by the algorithm in Sec. III.B.

C. Use of the Bundle Geometry for EMC Prediction

Once accurate spatial curve representation of the bundle geometry is obtained by the proposed algorithms, EMC performance can be predicted via full-wave or, alternatively, by MTL modeling. As a matter of fact, several 3D full-wave electromagnetic solvers are equipped with built-in functions to import spatial analytical curves in the form of wire coordinate expressions as functions of a variable t, that is, $[x(t), y(t), z(t)]$. In the remainder of this work, the predictions obtained by full-wave simulation will be taken as reference in order to investigate the accuracy achievable through MTL modeling via the UCS technique. This is done in the perspective to use the proposed algorithms to generate several bundle samples so to provide statistical estimates of the EMC performance of the system composed of the bundle under analysis and the relevant terminal units. In light of this, the proposed MTL-model will also be compared in terms of prediction accuracy and numerical efficiency versus the model in [1], where a significantly coarser digitization, leading to unavoidable discontinuities in the wire trajectories as large as a wire diameter, is adopted to maximize computational efficiency.

In passing, it is worth underlining that validity of MTL theory is not taken for granted in the specific application examples presented in the following sections. As a matter of fact, in contrast with previous studies, where the average height above ground was assumed to be much larger than wire separation [1], [15], the bundles considered in this work exhibit minimum distance from the ground plane. Hence, if on the one hand such a reduced height extends the maximum frequency of applicability of MTL theory (according to the rule-of-thumb $h < \lambda_{\min}/10$, [10]) to the gigahertz range, on the other hand this exacerbates line non-uniformity. As a consequence, the assumption of Transverse Electro-Magnetic (TEM) propagation is not strictly satisfied in some cases.

IV. Crosstalk Prediction

For crosstalk analysis, one wire (generator) inside the bundle is assumed to be driven by a non-ideal voltage source, and the voltages induced across the terminations of the other wires (receptors) are predicted. In the proposed examples, two cable bundles are considered satisfying the assumptions of loose and tight bundle previously introduced. To this end, geometrical characteristics of the bundles under analysis are chosen as follows: Number of wires $N = 7$, longitudinal length $L = 1$ m, inner wire radius $r_{\mathrm{w}} = 0.25$ mm, outer wire radius $r = 0.5$ mm. For the sake of simplicity, yet without loss of generality, bare wires are considered here, that is a unitary relative permittivity $\varepsilon_r = 1$ is assigned to the dielectric coating. Moreover, the ratio between the wire separation, s, and the wire radius, r, is set equal to $s/r = 6$ in the loose bundle, and equal to $s/r = 2.5$ in the tight one. This difference

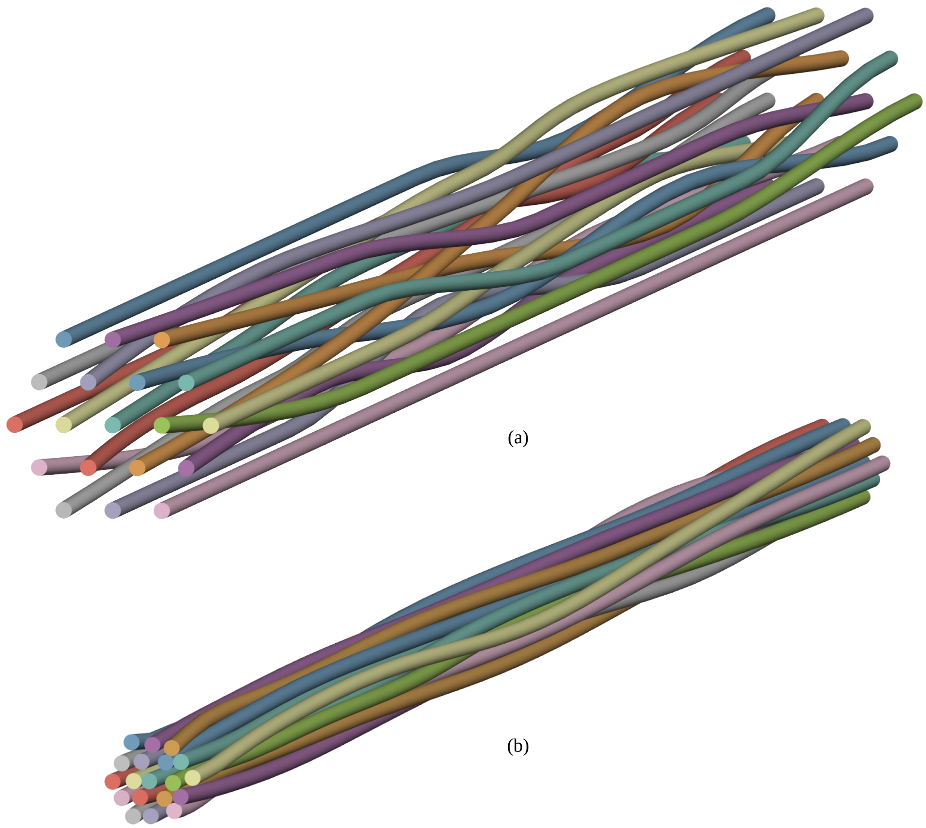

Fig. 4. Examples of (a) loose, and (b) tight bundles generated via the algorithms in Sec. III.A and Sec. III.B, respectively (see text for details). The bundle geometries are constructed by importing the spatial curves into a 3D EM simulator, and then rendered in the embedded CAD tools.

implies a different average height above ground of the two bundles, here chosen as $h = 3.5$ mm in the former case (loose bundle), and $h = 2.5$ mm in the latter one (tight bundle).

The geometry of the loose bundle is generated via the simplified algorithm in Sec. III.A, assuming 10 sections with length $L_s = 10$ cm. Each wire in the bundle is described by 20 piece-wise cubic interpolation functions, i.e., 10 for the x- and 10 for the y-coordinate. The same section length is assumed also for the tight random bundle, whose geometry is conversely generated resorting to the enhanced algorithm in Sec. III.B.

A. Crosstalk in a Single-Ended Receptor Circuit

To analyze crosstalk in a single-ended receptor circuit, the terminal sections illustrated in Fig. 5(a) are adopted, where each wire is connected to ground through (nearly matched) resistors of 150 Ω. Other termination values were considered within this study, but the results are here omitted for brevity, as the comparison between MoM and MTL solution is generally less critical than in the case of matching. Examples of the obtained results are plotted in Fig. 6. Green and black curves were obtained by the bundle geometry generated by the proposed algorithms. In the former case (green curves), the model was imported into a MoM-based solver. In the latter (black curves), the solution was obtained by MTL modeling (UCS technique), by splitting the bundle into 200 uniform sub-sections. This number was selected as a trade-off between accuracy and computational efficiency. Specifically, the MTL solution costs merely about 10 s, while for the MoM solution at least 40 minutes are required.

These results are also compared versus the prediction (red curves) obtained by the modeling technique proposed in [1]. To this end, the involved reference cross sections were selected according to a minimum distance mapping algorithm [5], [7]. More specifically, Fig. 6(a) shows the voltage induced at the near end of wire #6, in the loose bundle. The other plots in Fig. 6 were obtained for the tight bundle. Particularly, Fig. 6(b) and Fig. 6(d) show the crosstalk voltages induced across one termination of two general wires in the bundle. A linear-scale for the frequency was adopted in Fig. 6(d) in order to better appreciate the comparison in the interval from 1 to 5 GHz. Finally, Fig. 6(c) shows the voltage at the far end of the wire driven by the voltage source (i.e., wire #1).

The very good agreement between the green and black curves proves effectiveness of MTL modeling combined with the UCS technique in predicting crosstalk in a wire bundle even in the presence of significant non-uniformity affecting the bundle geometry with respect to ground. Further, the non-negligible discrepancies with respect to the outcomes of the model in [1] (red curves) confirm the need for precise modeling and digitization of the bundle geometry if accurate crosstalk prediction is the target.

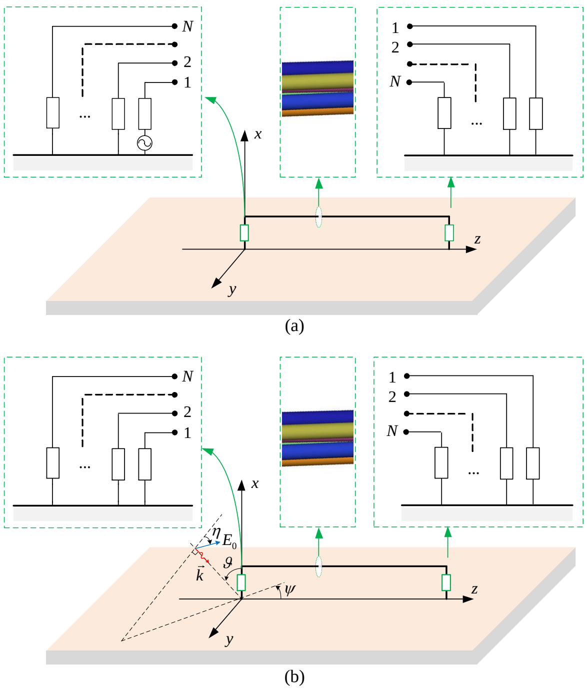

Fig. 5. Structures under analysis for (a) crosstalk and (b) field-to-wire coupling prediction.

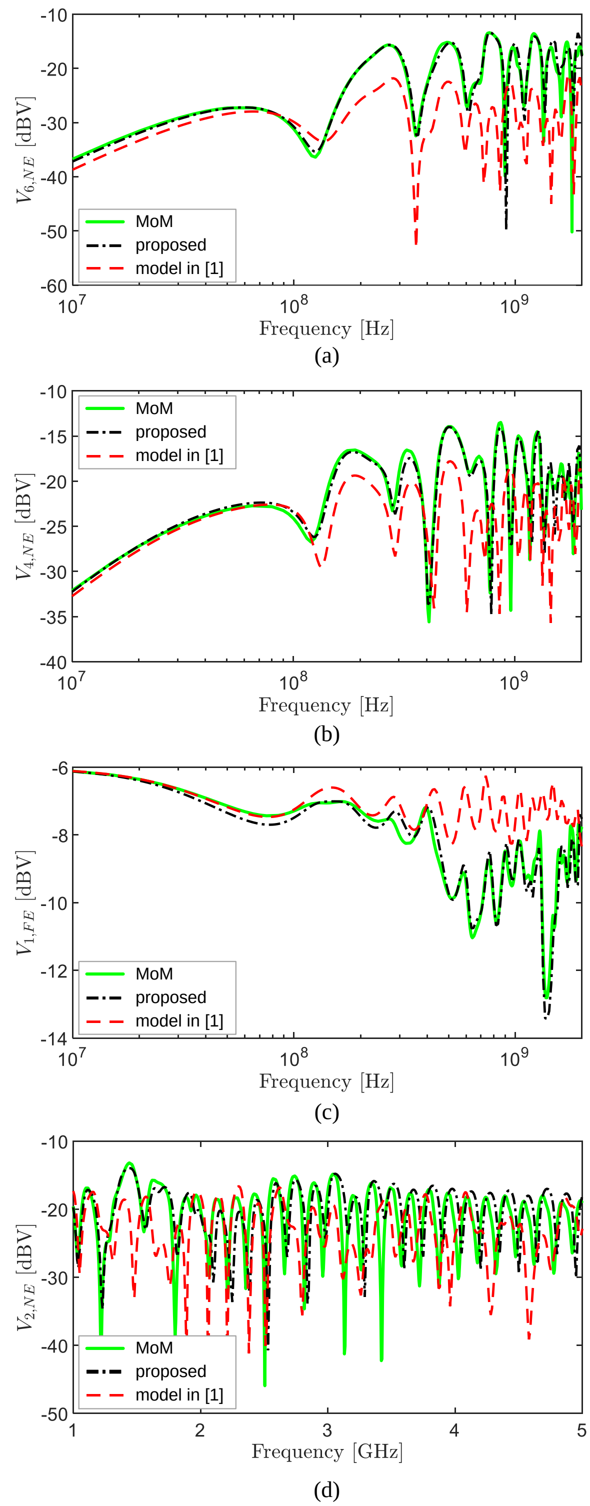

Fig. 6. Crosstalk prediction: Voltages induced at terminations of the (a) loose, and (b)-(d) tight bundles under analysis (see Sec. IV.A).

B. Crosstalk in a Differential Wire-Pair

In order to illustrate accuracy of the proposed technique for the prediction of crosstalk in differential wire-pairs (typically more critical than predictions involving just the common-mode, [1]), a pair of wires within the bundle is assumed to be operated as a differential line, and accordingly terminated in $150\ \Omega$ resistors as shown in Fig. 7(a). The crosstalk voltages induced across the differential line loads are then predicted by exploiting the proposed bundle geometry in combination with MoM (green curves) and MTL theory (black curves), and compared versus the prediction obtained by the model in [1] (red curves). Examples of results are shown in Fig. 8. For the sake of a better comparison of the outcomes, a logarithmic scale is adopted for the frequency interval up to 2 GHz (first panel), whereas a linear scale is used for the interval from 1 GHz to 5 GHz (second panel). Unlike MTL predictions obtained by the proposed bundle geometry, those obtained by the bundle model in [1] reveals significant differences (more than 10 decibels) in both frequency intervals shown. This result further confirms the need of a physically-based bundle model combined with proper digitization of the bundle geometry as far as accurate prediction of crosstalk is required.

V. Field-to-Wire Coupling Prediction

This section focuses on the prediction of voltages and currents induced in the terminal loads of a bundle, illuminated by an electromagnetic field. To this end, the two bundle geometries (loose and dense bundle, respectively) introduced in Section IV are considered. General conditions of polarization and direction of incidence are assumed for the uniform plane-wave field impinging upon the bundle. With reference to Fig. 5(b), the electric-field strength is $E_0 = 1$ V/m, the wave elevation angle is $\vartheta = 50°$, the azimuth angle is $\psi = 20°$, and the polarization angle is $\eta = 60°$.

For MTL analysis, the field-to-wire coupling model in [15] is adopted, and the outcomes are compared versus those obtained via full-wave simulation. However, unlike in [15], the effects due to the vertical risers (i.e., the wire segments

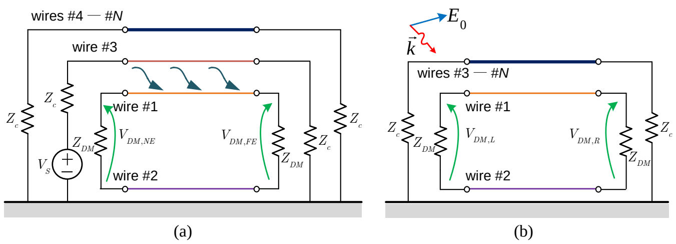

Fig. 7. Terminal networks used to investigate (a) crosstalk and (b) field-to-wire coupling in a differential wire-pair.

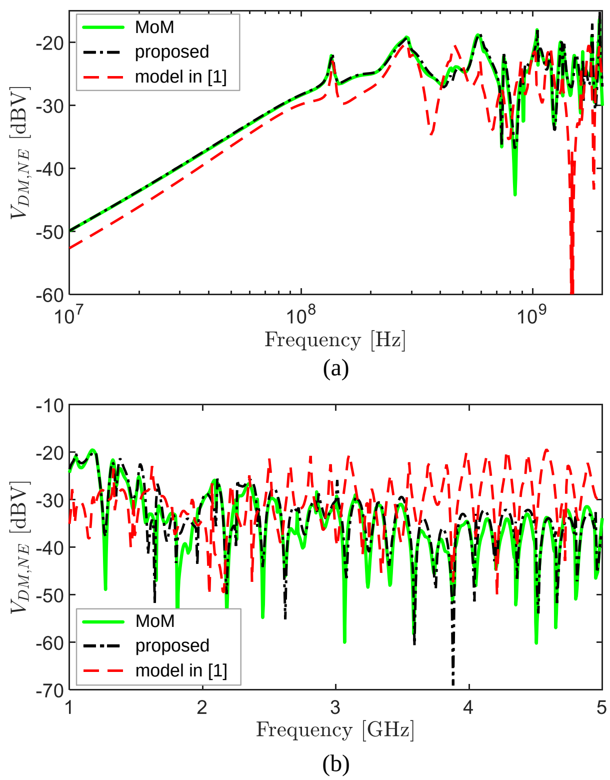

Fig. 8. Crosstalk prediction: DM voltage at the near end of a differential wire-pair inside the (a) loose and (b) tight bundle under analysis (see Sec. IV.B).

connecting the bundle ends to ground) are here disregarded. Indeed, preliminary simulations revealed negligible coupling with the terminal risers in the frequency interval up to 5 GHz, due to the extremely low height above ground of the bundle under analysis.

A. Field Coupling to a Single-Ended Circuit

In the first test case, all the wires inside the bundle are individually connected to ground by 150 Ω resistances. Full-wave and MTL model simulations were carried out both for the loose and the dense bundle introduced in Section IV. Examples of results are shown in Figs. 9(a)-(c), where the currents induced in the terminations of selected wires in the bundle are plotted for frequencies up to 5 GHz.

The comparison versus full-wave simulations (green curves) shown in Figs. 9(a),(b) confirms the accuracy of the MTL-UCS model using the bundle geometry generated via the proposed approach (black curves). Conversely, a twofold conclusion can be drawn from the comparison versus the curves generated by the approximate model in [1], [2]. For frequencies up to approximately 500 MHz, the predictions obtained by [1], [2] accurately reproduce the induced currents. In this frequency interval the solution seems to be less sensitive to accurate modeling and digitization of the wire bundle with respect to what previously observed in the case of crosstalk. In contrast, significant discrepancies are observed for frequencies above 500 MHz, confirming the limitation of such a simplified representation. Indeed, the sharp peaks observed in the gigahertz range are spurious effects to be ascribed to the reflections occurring at the abrupt transitions between the adjacent sections the bundle was split into.

To better investigate this phenomenon, an additional dense bundle with reduced section length ($L_s = 5$ cm) is generated and used for simulation. The obtained results are compared versus those of the bundle with longer section-length ($L_s = 10$ cm) in the plots of Figs. 9(c),(d). Comparison of the two plots confirms the spurious nature of the observed peaks, pointing out correlation between the frequencies of the peaks and the section length used to generate the bundle. Namely, if the section length decreases (in this example from 10 cm to 5 cm, thus increasing the number of sections from 10 to 20), the observed peaks shift towards higher frequencies (in the specific example, the first peak shifts from 1.5 GHz to 3 GHz.)

B. Field Coupling to a Differential Wire-Pair

To assess model accuracy in predicting differential-mode quantities, a wire-pair in the bundle is assumed to be operated as a differential line, with the line terminations set as shown in Fig. 7(b), and the differential-mode voltage induced across the line termination at the right end is predicted both for the loose and the dense bundle. The results are shown in Fig. 10(a) and 10(b), respectively.

Comparison versus full-wave simulation further confirms the accuracy of the MTL-UCS solution exploiting the proposed bundle geometry, whereas significant discrepancies (on the order of several decibels) are observed with respect to the model in [1], even just above 100 MHz. As pointed out in Sec. V.A, the prediction accuracy of such a simplified model further degrades in the gigahertz range, where the frequency response of the differential-mode voltage exhibits spurious peaks.

VI. Conclusion

In this work, a new model has been proposed for the generation of physically-based trajectories of wire in bundles, where random wire displacements and interchanges occur due to hand-assembling. By representing the wire trajectories through analytical curves able to preserve the smoothness of the wires' paths and the bundle compactness, some of the limitations of the models currently available in the literature are overcome.

Full-wave electromagnetic simulation (based on MoM), carried out importing the bundle geometry generated by the proposed model, were used as the reference solution to assess

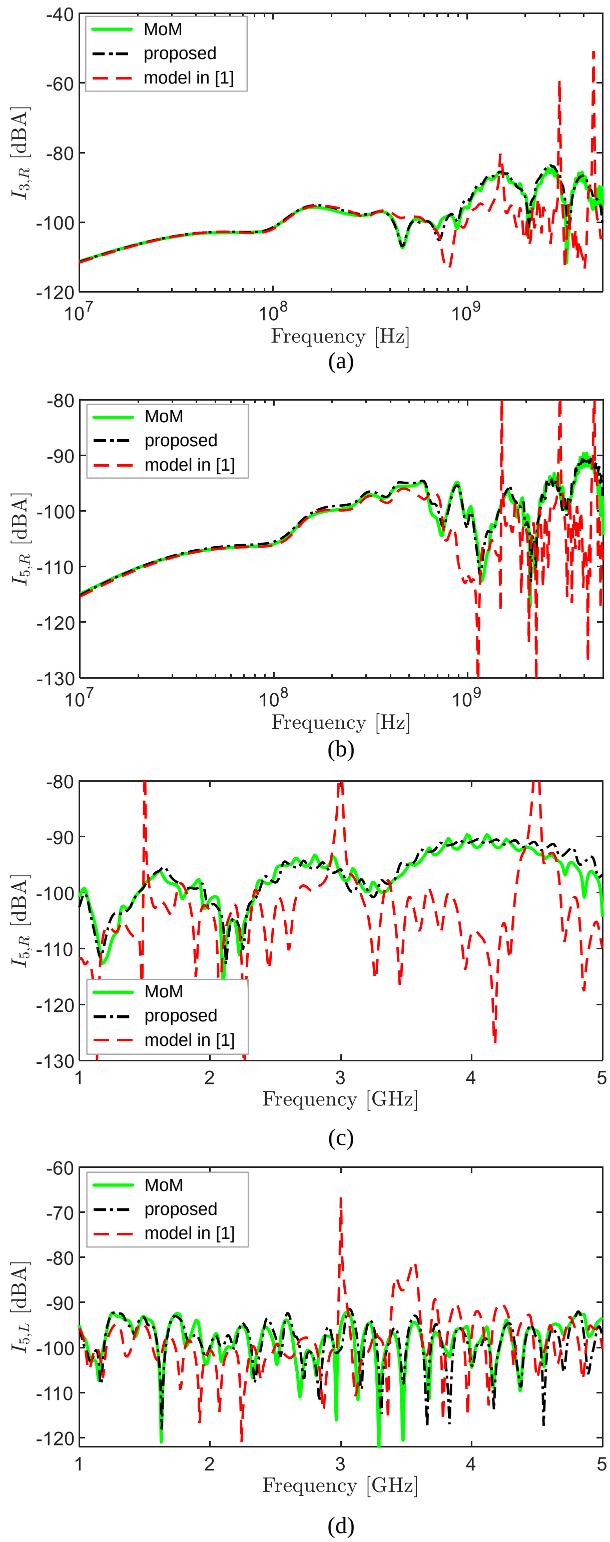

Fig. 9. Field-to-wire coupling prediction: Voltages induced across the terminations of the (a) loose bundle, (b)-(c) tight bundle with section length $L_s = 10$ cm, and (d) tight bundle with section length $L_s = 5$ cm (see Sec. V.A).

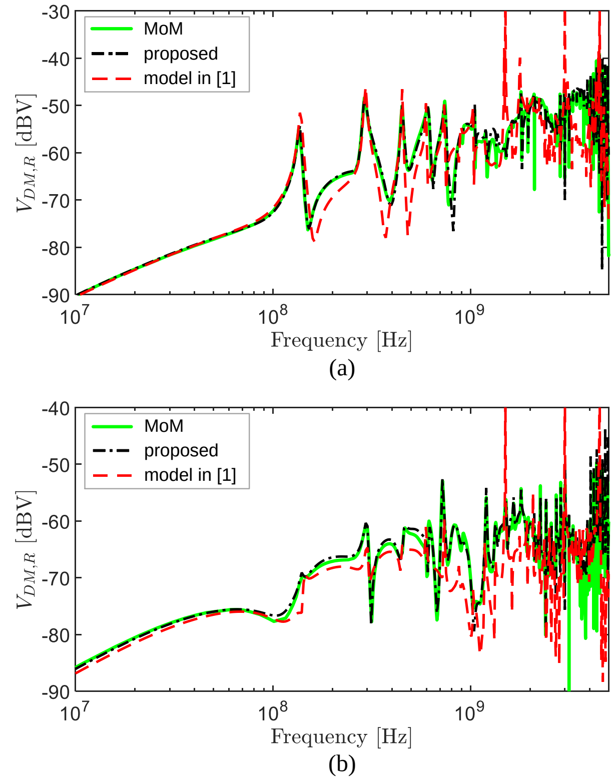

Fig. 10. Field-to-wire coupling prediction: Differential-Mode voltage at the right end of a differential wire-pair inside the (a) loose and (b) tight bundles under analysis (see Sec. V.B).

the prediction accuracy that can be achieved by MTL modeling combined with the UCS technique, despite the strong non-uniformity possibly affecting the wiring structure (when the bundle is laid very close to ground).

The proposed model was used to predict the noise induced in the bundle terminal units by crosstalk and field-to-wire coupling. Then, the obtained predictions were compared versus the outcomes of the approximate MTL model in [1], employing a less accurate representation and digitization of the bundle in order to minimize the computational cost. The comparison shows that the proposed bundle model outperforms the previous model in [1] in terms of accuracy, either for crosstalk and for field-to-wire coupling prediction. Namely, as far as crosstalk is concerned, the model in [1] exhibits discrepancies w.r.t. MoM larger than 10 decibels. In the prediction of field-to-wire-coupling, it introduces spurious resonances in the gigahertz range, due to reflections at the transitions between adjacent bundle segments, where wire discontinuities as large as a wire diameter are necessary introduced by the generation algorithm. In view of the need of repeated-run simulations (strictly required for statistical EMC modeling), it is important to note that increasing prediction accuracy was achieved at the price of a larger computational cost. However, this appears to be acceptable. Indeed, in the proposed examples, the time to generate one dense bundle sample (with $N_s = 10$ segments) on a desktop PC was on the order of 3 minutes (this time is negligible in [1]). For MTL solution, enhancing bundle digitization from 10 (number of segments here used for the approximate model, in [1]) to 200 segments (proposed model) determined an increase in computational time from 0.86 s to 10.30 s for crosstalk simulation, and from 2.77 s to 10.61 s for the example on field-to-wire-coupling. Eventually, computation of the per-unit-length matrix parameters (by the method in [16]) for 201 cross-sections further increased the computational time by 18 s. This time is negligible in [1], since only specific wire positions are available in the reference cross-section. These are (average) unitary times for the generation and simulation of a bundle sample.

Although not considered here for the sake of simplicity, it is also worth mentioning that inclusion of wire coating in the proposed model can be readily accomplished without additional computational efforts for bundle digitization. Besides, the proposed framework can be readily extended to model random bundles of twisted-wire pairs (TWPs). In this case, the algorithm can be used to describe the trajectory of the TWP axis, and the two wires in the TWP can be afterwards represented as an ideal or real helix around the TWP axis.

REFERENCES

[1] G. Spadacini, F. Grassi, and S. A. Pignari, "Field-to-wire coupling model for the common mode in random bundles of twisted-wire pairs," *IEEE Transactions on Electromagnetic Compatibility*, vol. 57, no. 5, pp. 1246–1254, 2015.

[2] S. A. Pignari, G. Spadacini, and F. Grassi, "Modeling field-to-wire coupling in random bundles of wires," *IEEE Electromagnetic Compatibility Magazine*, vol. 6, no. 3, pp. 85–90, 2017.

[3] S. Salio, F. Canavero, J. Lefebvre, and W. Tabbara, "Statistical description of signal propagation on random bundles of wires," in *13th Int. Zurich Symp. Electromagn. Compat, Zurich, Switzerland*, 1999.

[4] S. Salio, F. Canavero, D. Lecointe, and W. Tabbara, "Crosstalk prediction on wire bundles by Kriging approach," in *Electromagnetic Compatibility, 2000. IEEE International Symposium on*, vol. 1. IEEE, 2000, pp. 197–202.

[5] S. Sun, G. Liu, J. L. Drewniak, and D. J. Pommerenke, "Hand-assembled cable bundle modeling for crosstalk and common-mode radiation prediction," *IEEE Transactions on electromagnetic compatibility*, vol. 49, no. 3, pp. 708–718, 2007.

[6] C. Jullien, P. Besnier, M. Dunand, and I. Junqua, "Towards the generation of industrial bundles through a random process under realistic constraints," in *EMC Europe 2010 9th International Symposium on EMC joint with 20th International Wroclaw Symposium on EMC*, 2010, pp. page–97.

[7] D. Bellan and S. A. Pignari, "Efficient estimation of crosstalk statistics in random wire bundles with lacing cords," *IEEE Transactions on Electromagnetic Compatibility*, vol. 53, no. 1, pp. 209–218, 2011.

[8] C. Jullien, P. Besnier, M. Dunand, and I. Junqua, "Crosstalk analysis in complex aeronautical bundle," in *Electromagnetic Compatibility (EMC EUROPE), 2013 International Symposium on*. IEEE, 2013, pp. 253–258.

[9] C. R. Paul and J. W. McKnight, "Prediction of crosstalk involving twisted pairs of wires-Part I: A transmission-line model for twisted-wire pairs," *IEEE Transactions on Electromagnetic Compatibility*, no. 2, pp. 92–105, 1979.

[10] C. R. Paul, *Analysis of multiconductor transmission lines*. John Wiley & Sons, 2008.

[11] A. Shoory, M. Rubinstein, A. Rubinstein, C. Romero, N. Mora, and F. Rachidi, "Application of the cascaded transmission line theory of Paul and McKnight to the evaluation of NEXT and FEXT in twisted wire pair bundles," *IEEE Transactions on Electromagnetic Compatibility*, vol. 55, no. 4, pp. 648–656, 2013.

[12] I. Castillo, F. J. Kampas, and J. D. Pintr, "Solving circle packing problems by global optimization: numerical results and industrial applications," *European Journal of Operational Research*, vol. 191, no. 3, pp. 786–802, 2008.

[13] C. De Boor, *A practical guide to splines*. Springer-Verlag New York, 1978, vol. 27.

[14] F. N. Fritsch and R. E. Carlson, "Monotone piecewise cubic interpolation," *SIAM Journal on Numerical Analysis*, vol. 17, no. 2, pp. 238–246, 1980.

[15] G. Spadacini, F. Grassi, F. Marliani, and S. A. Pignari, "Transmission-line model for field-to-wire coupling in bundles of twisted-wire pairs above ground," *IEEE Transactions on Electromagnetic Compatibility*, vol. 56, no. 6, pp. 1682–1690, 2014.

[16] J. C. Clements, C. R. Paul, and A. T. Adams, "Computation of the capacitance matrix for systems of dielectric-coated cylindrical conductors," *IEEE Transactions on Electromagnetic Compatibility*, no. 4, pp. 238–248, 1975.

Xiaokang Liu received the Double M.Sc. degree in electrical engineering from Xi'an Jiaotong University, Shaanxi, China, and Politecnico di Milano, Italy, in 2016. Since November 2017, he has been working toward the Ph.D. degree in electrical engineering at Politecnico di Milano, Italy.

His research interests include electromagnetic compatibility, power electronics and signal integrity.

Flavia Grassi (M'07-SM'13) received the Laurea (M.Sc.) and Ph.D. degrees in electrical engineering from Politecnico di Milano, Milan, Italy, in 2002 and 2006, respectively.

She is currently an Associate Professor in the Department of Electronics, Information and Bioengineering, Politecnico di Milano. From 2008 to 2009, she was with the European Space Agency (ESA), ESA/ESTEC, The Netherlands, as a Research Fellow. Her research interests include distributed-parameter circuit modeling, statistical techniques, characterization of measurement setups for EMC testing (aerospace and automotive sectors), and application of the powerline communications technology in ac and dc lines.

Dr. Grassi received the International Union of Radio Science (URSI) Young Scientist Award in 2008, and the IEEE Young Scientist Award at the 2016 Asia-Pacific International Symposium on EMC (APEMC), the IEEE EMC Society 2016 Transactions Prize Paper Award, and the Best Symposium Paper Awards from the 2015 Asia-Pacific Int. Symp. on EMC (APEMC) and the 2018 Joint IEEE EMC & APEMC Symposium.

Giordano Spadacini (M'07–SM'16) received the Laurea (M.Sc.) and Ph.D. degrees in electrical engineering in 2001 and 2005, respectively, from Politecnico di Milano, Italy, where he is currently an Associate Professor with the Dept. of Electronics, Information and Bioengineering. His research interests include statistical models for the characterization of interference effects, distributed parameter circuit modeling, experimental procedures and setups for EMC testing, and EMC in aerospace, automotive and railway systems.

Dr. Spadacini is a recipient of the 2005 EMC Transactions Prize Paper Award, the 2016 Richard B. Schulz Best EMC Transactions Paper Award, two Best Symposium Paper Awards from the 2015 Asia-Pacific Int. Symp. on EMC (APEMC) and the 2018 Joint IEEE EMC & APEMC Symposium.

Sergio A. Pignari (M'01–SM'07–F'12) received the Laurea (M.S.) and Ph.D. degrees in electronic engineering from Politecnico di Torino, Turin, Italy, in 1988 and 1993, respectively.

From 1991 to 1998, he was an Assistant Professor with the Dept. of Electronics, Politecnico di Torino, Turin, Italy. In 1998, he joined Politecnico di Milano, Milan, Italy, where he is currently a Full Professor of Circuit Theory and Electromagnetic Compatibility (EMC) at the Dept. of Electronics, Information, and Bioengineering, and Chair of the board of B.Sc. and M.Sc. Study Programmes in Electrical Engineering, term 2015-20. He is the author or coauthor of more than 200 papers published in international journals and conference proceedings. His research interests are in the field of EMC and include field-to-wire coupling and crosstalk, conducted immunity and emissions in multi-wire structures, statistical techniques for EMC prediction, and experimental procedures and setups for EMC testing.

Dr. Pignari is co-recipient of the 2005 and 2016 IEEE EMC Society Transactions Prize Paper Award, and a 2011 IEEE EMC Society Technical Achievement Award. He is currently serving as an Associate Editor of the IEEE TRANSACTIONS ON ELECTROMAGNETIC COMPATIBILITY. From 2010 to 2015 he served as the IEEE EMC Society Chapter Coordinator. From 2007 to 2009 he was the Chair of the IEEE Italy Section EMC Society Chapter. He has been Technical Program Chair of the ESA Workshop on Aerospace EMC since 2009, and a Member of the Technical Program Committee of the Asia Pacific EMC Week since 2010. He is a member of the International Academic Committee of The State Key Laboratory of Electrical Insulation and Power Equipment (SKLEIPE) at Xi'an Jiaotong University (XJTU), Xi'an, China, term 2015-20.